Evaluation of the Shear Strength Capacity of Precast-Prestressed Hollow Core Floor Slabs – Part 2: Code Comparisons and Design Method

E. Brunesi
ROSE Programme, UME School, IUSS Pavia, Italy

D. Bolognini & R. Nascimbene
European Centre for Training and Research in Earthquake Engineering (Eucentre), Pavia

SUMMARY:
Shear strength of precast prestressed concrete hollow core slab cross sections with circular and non-circular voids has been evaluated for 200, 265, 320, 370, 400 and 500 mm thick slab, numerically and experimentally. Shear stress distribution and crack patterns are predicted through refined non-linear finite element analyses, matching experimental test data collected from past programs. A comparison with American Concrete Institute (ACI), Eurocode 2 (EC2) and Canadian Standards Association (CSA) specifications has been carried out.
Experimental and numerical results highlight that shear strength evaluated by ACI, EC2 and CSA specifications is often conservative for circular voids cross sections, while ACI and EC2 predictions are not conservative for deeper slab sections with flat webs. However, CSA predictions for all types of hollow core slab sections are more conservative than ACI and EC2 predictions. An alternative and conservative design method has been proposed to predict shear strength of these no-transverse reinforcement members.

Keywords: Hollow core slab; Shear strength; Prestressed concrete; Precast members; Circular Voids

1. CAMPAIGN OF NUMERICAL ANALYSES

Research works available in literature [Pajari, 2005; Hawkins and Ghosh, 2006] demonstrated that precast-prestressed hollow core slab units with deep cross sections, longer supports and higher line loads acting close to the supports, are subjected to initial web shear cracking at the end regions that leads to critical brittle web-shear failure mechanisms. It was recognized that these members without transverse reinforcement can fail, due to web-shear cracking in the end regions, at loads less than those predicted by traditional Codes approaches (EC2, ACI). Hence, the shear strength capacity of these members without transverse reinforcement, characterized by intrinsic lack of ductility reserves, is evaluated through a campaign of detailed non-linear three-dimensional finite element analyses, matching experimental test data collected from past experimental programs, performed at VTT on extruded units [Pajari, 2005]. The experimental test protocol, based on the application of a pseudo-static vertical load, monotonically increased till the shear failure mechanism is reached, has been numerically reproduced, highlighting that the experienced brittle web-shear failure mechanism is governed by hollow core shapes (circular and non-circular), related web width variation along depth and concrete thickness above and below the hollow core, as evidenced by the evolution of the principal tensile strain distributions, the relative crack pattern and shear stress distributions. The presence of a variable inclined strut, whose width and inclination angle evolves, as the imposed vertical displacement increases, according to hollow core shapes and the relative web width variation along depth, clearly emerges from the evolution of principal tensile and compressive strain distributions, shear stress distributions and relative crack pattern. Strut width reduces increasing the imposed displacement, reproducing the actual shear stress flow, characterized by the peaks placed in correspondence of the bottom side of the cross-section, rather than at the level of the centroid. The reliable, robust, stable and general modeling approach, based on non-linear fracture model, which allows for post-cracking redistribution, reproducing the actual stress path, was adopted to perform sensitivity analyses, varying prestress distribution along strands and loss of prestress ratios to quantify their influence on the structural response.

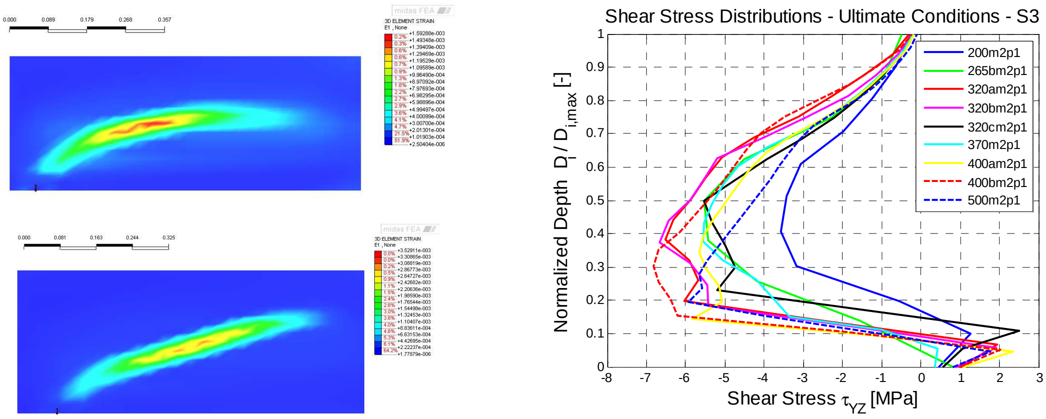

Figure 1.1 Comparison between principal tensile strain of circular (Specimen320c) and non-circular voids (Specimen320b) hollow core units and shear stress distributions close the support (x/D < 0.4)

Starting from the emerged scenario, the principal target of this work is to develop useful, conservative, accurate and simple analytical tools and practical provisions to properly evaluate the shear strength capacity of hollow core units for any type of geometry, cross-section shape (with circular and non-circular voids) and prestress levels. Hence, experimentally observed shear strength capacities are predicted according to three codes approaches (EC2, ACI and CSA) and a simple design method against web shear failure mechanism, proposed by Yang [1994], in which shear stresses are directly derived from Navier's theory, taking into account the contribution due to the transfer of the prestress force. To quantify their effectiveness, highlighting their under/over-conservatism levels, comparison with experimental data will be deeply discussed, pointing out trends evidenced by each approach.

2. CODES AND RESEARCH DESIGN APPROACH AGAINST WEB-SHEAR FAILURE

A brief review of three of the most commonly known Codes provisions (EC2, ACI and CSA) for shear design against web-shear failure mechanism has been developed, emphasizing the assumptions on which they are based.

2.1 Eurocode 2 (EC2)

EC2 prescribes that, in prestressed single span members without shear reinforcement, for regions uncracked in bending, the shear strength capacity should be limited by the tensile concrete strength, through Eqn. 2.1:

$$V_{Rd,c} = \frac{Ib_w}{S}\sqrt{(f_{ctd})^2 + \alpha_1 \sigma_{cp} f_{ctd}} \tag{2.1}$$

where I is the second moment of area, b_w is the width of the cross-section at the centroidal axis, allowing for the presence of ducts, S is the first moment of area above and about the centroidal axis, α_1 is equal to $l_x/l_{pt2} \leq 1.0$ for pretensioned tendons, l_x is the distance of section considered from the starting point of the transmission length, l_{pt2} is the upper bound value of the transmission length of the prestressing element and σ_{cp} is the concrete compressive stress at the centroidal axis due to prestressing ($\sigma_{cp}=N_{Ed}/A_c$, N_{Ed}>0 in compression). Maximum principal tensile stress criterion failure is adopted and the evaluation of the shear strength capacity is based on the assumption that the maximum web-shear cracking stress is expected to occur at the centroidal axis level.

2.2 American Concrete Institute (ACI)

In Section 11.4.3 of ACI, the shear force V_u is limited to the lesser between φV_{ci} and φV_{cw}, where V_{ci} and V_{cw} are the flexure-shear cracking strength and the web-shear cracking one, while φ is 0.75. ACI Code recommends that the principal tensile stress at web-shear cracking be taken as $0.33(f'_c)^{0.5}$. Moreover, it is recommended that V_{cw} can be computed as the shear force corresponding to dead and live loads that result in a principal tensile stress at the centroidal axis of member equal to the value suggested by ACI Code. However, in order to evaluate the shear strength capacity of prestressed concrete members against web-shear cracking failure mechanisms, ACI permits the use of an approximate expression, given by Eqn. 2.2.

$$V_{cw} = (0.29\sqrt{f_c^{'}} + 0.3 f_{pc}) b_w d + V_p \qquad \text{MPa units} \tag{2.2}$$

where d is the distance from extreme compression fiber to the centroid of prestressing steel, b_w is the web width, f_{pc} is the compressive stress in the concrete at the centroid of the cross-section ($f_{pc}=P/A$), f'_c is the specified compressive strength of concrete and V_P is the vertical component of the effective prestress force. It is also recommended by ACI Code that d need not be taken as less than $0.8h$ where h is the overall thickness of the slab including any eventual composite topping. Because of concern with the applicability of these empirical equation to members made of high-strength concrete, the current version of ACI Code requires that the values of $(f'_c)^{0.5}$ used in all shear design equations be limited to 8.3 MPa. Section located less than a distance of $h/2$ from the face of the support can be designed for V_u (factored shear force at the section) computed at a distance $h/2$. This distance is often closer to the end of the member than the transfer length for prestressing steel strands. In such cases a reduced prestressing force has to be used in calculating V_{cw}, according to a linear distribution assumption. In section 11.4.4, it is prescribed that prestress force is assumed to vary linearly from 0 at the end of the slab unit to f_{pc} at the end of the transfer length, which is suggested to be taken as 50 diameters.

2.3 Canadian Standards Association (CSA)

The CSA Code, based on the Simplified Modified Compression Field Theory, SMCFT [Bentz *et al.*, 2006] which considers the post-cracking shear strength of the member, prescribes that the factored shear resistance shall be determined by Eqn. 2.3.

$$V_c = \phi_c \lambda \beta \sqrt{f_c^{'}}\, b_w d_v \tag{2.3}$$

where ϕ_c is a resistance factor for concrete, λ is a factor to account for low-density concrete, β is a factor accounting for shear resistance of cracked concrete, f'_c is the specified compressive strength of concrete, b_w is the minimum effective web width, d_v is the effective shear depth, taken as the greater of $0.9d$ or $0.72h$, where d is the distance from extreme compression fibre to centroid of longitudinal tension reinforcement, but need not be less than $0.8h$ for prestressed members and h is the overall thickness of the member. It is also prescribed that in the determination of V_c the term $(f'_c)^{0.5}$ shall not be taken greater than 8 MPa. From the clause 11.3.6.4 of the CSA, β can be determined as shown in Eqn. 2.4. The simplified method proposed by CSA implies that the specified yield strength of the longitudinal steel reinforcement does not exceed 400 MPa and the specified concrete strength does not exceed 60 MPa. Consequently, for the purposes of the research, the general method has to be adopted.

$$\beta = \frac{0.4}{(1+1500\varepsilon_x)} \cdot \frac{1300}{(1000+s_{ze})} \tag{2.4}$$

where ε_x is the longitudinal strain at mid-depth of the member due to factored loads and s_{ze} is the equivalent value of the crack spacing parameter, s_z, that allows for influence of aggregate size. The crack spacing parameter, s_z, depends on crack control characteristics of longitudinal reinforcement. ε_x and s_{ze} can be obtained from Eqn. 2.5 and 2.6, respectively.

$$\varepsilon_x = \frac{M_f / d_v + V_f - A_p f_{po}}{2(E_p A_p + E_c A_{ct})} \tag{2.5}$$

where M_f is the moment due to factored loads, V_f factored shear force, A_p area of prestressing tendons, f_{po} stress in prestressing tendons, E_p modulus of elasticity of prestressing tendons, E_c modulus of elasticity of concrete, A_{ct} area of concrete on flexural tension side of member. CSA prescribes that M_f and V_f shall be taken as positive quantities and M_f shall not be taken less than $(V_f - V_p)/d_v$. However, ε_x shall not be taken as less than $-0.2 \cdot 10^{-3}$.

$$s_{ze} = \frac{35 s_z}{15 + a_g} \tag{2.6}$$

where a_g is the maximum size of coarse aggregate. However s_{ze} shall not be taken as less than $0.85 s_z$ and the cracking spacing parameter shall be taken as d_v.

Both EC2 and ACI specifications are based on plane section assumption and Mohr circle theory, while CSA, based on the SMCFT, treats concrete as a diagonally shear cracked material and evaluate the aggregate interlocking as a function of the average tensile strength of concrete.

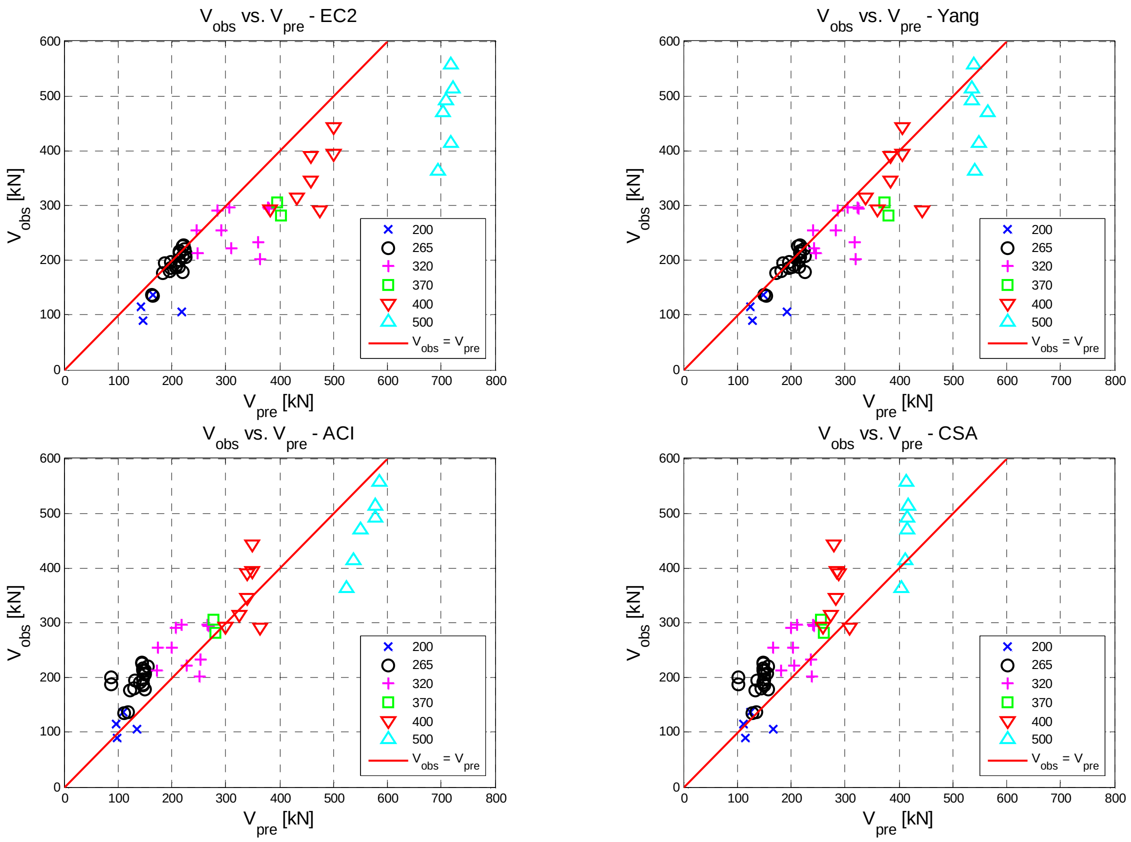

Figure 2.1 Experimentally observed, V_{obs}, vs. predicted, V_{pre}, shear strength capacity, for each nominal depth, according to EC2 provisions, Yang's design method, ACI and CSA recommendations, respectively

3 PROPOSED DESIGN APPROACH

To define a more appropriately conservative design approach, proposed to evaluate the shear strength capacity of precast-prestressed hollow core floor slab units, a critical review of the predictions, previously obtained by considering the four adopted methods, resulting from both Codes provisions

(EC2, ACI and CSA) and research work available in literature [Yang, 1994], is needed. Therefore, the ratio between experimentally observed and predicted shear strength capacity is graphed versus the following four dimensionless local geometric parameters, introduced to represent cross-sectional properties, according to Eqn. 3.1:

$$C_{t1} = \frac{t_{up}}{D} \qquad C_{t2} = \frac{t_{up}}{t_{low}} \qquad T_w = \frac{b_w}{D} \qquad C_S = \frac{A_{void}}{A_{circle}} \tag{3.1}$$

where C_{t1} can be defined as the ratio between the concrete thickness above the hollow core and the slab depth, C_{t2} is the ratio between the concrete thickness above and below the hollow core, T_w is the normalized web width with respect to the slab depth and C_S is a dimensionless hollow core shape factor, computed as the ratio between the area of the void and the area of the circle, obtainable from the nominal radius of each specimen type. Consequently, the main aim of this parameter is to describe the void type, both circular and non-circular, by only one equivalent non-dimensional coefficient; furthermore, it should be noticed that, according to each cross-section geometry type, this factor can reach values even higher than one, since the defined equivalent circle is not always inscribed in its relative non-circular void, particularly for what concerns deeper hollow core cross-sections (400 and 500 mm deep slab units). This approach, aimed at a critical review of the adopted methods, is also addressed to investigate if some general, global and robust tendencies can be established between the evidenced mismatch and some local geometric factors.
In Figure 3.1, the ratios between observed and predicted shear strength capacity, V_{obs}/V_{pre}, according to EC2 provisions and 5% loss of prestress ratio, are plotted versus the introduced local cross-sectional geometric factors, C_{t1}, C_{t2}, T_w and C_S, respectively.

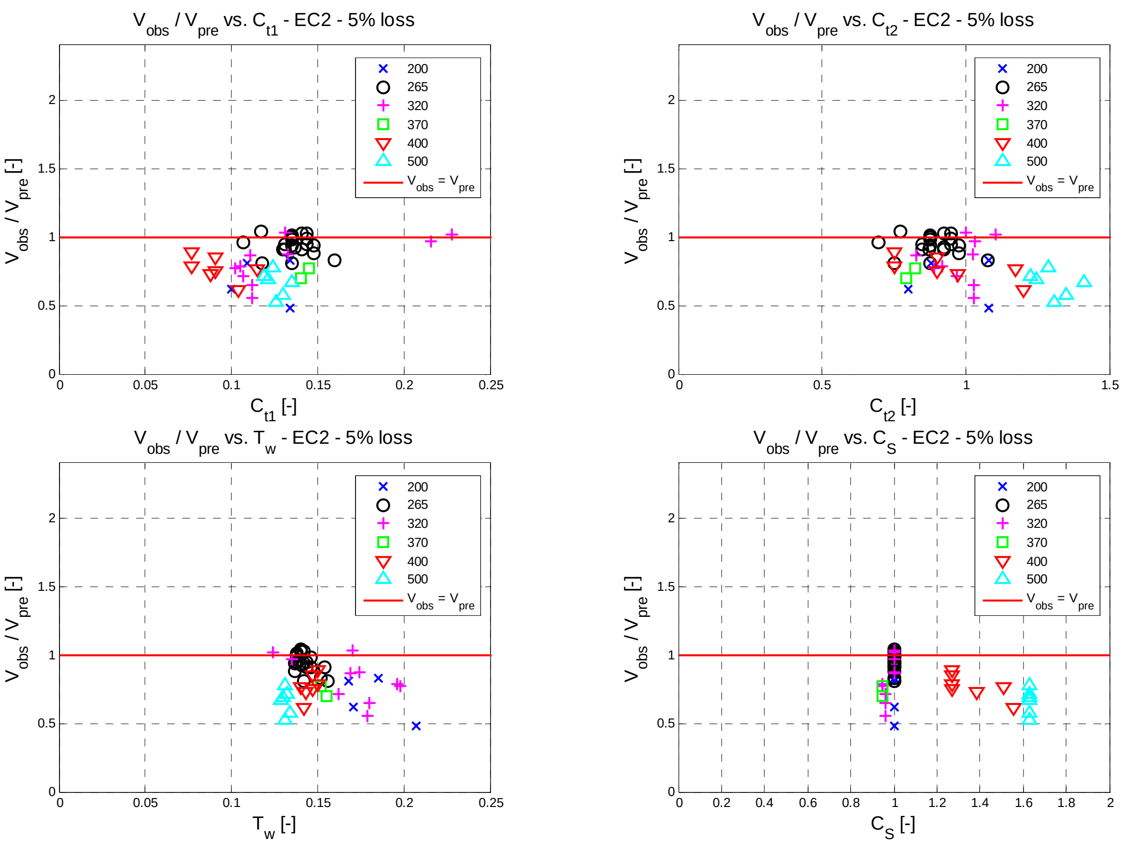

Figure 3.1 Ratio between observed and predicted shear strength capacity, V_{obs}/V_{pre}, according to EC2 provisions and 5% loss of prestress ratio, vs. local cross-sectional geometric factors, C_{t1}, C_{t2}, T_w and C_S, respectively

For what concerns EC2 predictions, no significant and robust trends can be extrapolated with respect to any of the considered dimensionless coefficients; the presence of evident scatter can be clearly

identified and no tendencies with respect to the nominal depth or the normalized hollow core shape factor can be appreciated. Negligibly reduced scatter, if compared to EC2 provisions, is achieved by Yang's predictions, anyway avoiding any type of reasonable and consistent correlation between the experimental-analytical mismatch and the introduced local geometric parameters. Similar considerations can be drawn for both ACI and CSA provisions, which are even characterized by an increased dispersion of the predictions with respect to the dimensionless geometric variables. Hence, the discrepancy between the considered approaches and the experimental data seems to be independent with respect to the four introduced parameters. Similar considerations can be drawn for each approach (EC2, Yang, ACI and CSA), if 15% loss of prestress is assumed.
The proposed approach basically consists in a critical review of EC2 prescriptions, according to the introduction of corrective coefficients, developed to properly take into account cross-section geometric characteristics, in terms of dimensionless local geometric parameters related to hollow core shapes. As evidenced, no reasonable and direct correlation can be established between the experimental-analytical mismatch and the previously defined geometric factors. In fact, the dimensionless hollow core shape factor, C_S, is a global parameter, based on the ratio between areas; consequently, it cannot properly capture the effect of the hollow core shape, particularly in terms of web width variation along depth, which, as highlighted by the performed campaign of refined non-linear solid finite element analyses, was proved to evidently affect the response of precast-prestressed hollow core slab units, governing the evolution of shear stress, principal tensile and compressive strain distributions, crack pattern and, hence, experienced brittle web-shear failure mechanism. Consequently, the proposed design approach can be formulated according to Eqn. 3.2, based on the adoption of the maximum principal tensile stress criterion failure, which implies that the concrete cracks if the maximum principal stress in the web reaches the cracking stress (uniaxial concrete tensile stress). The proposed expression can be easily deduced according to this assumption, combined with Mohr's circle theory.

$$V_{Rd,c} = \frac{Ib_w}{SC_{HCS}} \sqrt{(f_{ctm})^2 + \alpha_1 \sigma_{cp} f_{ctm}} \tag{3.2}$$

where I is the second moment of area, b_w is the width of the cross-section at the centroidal axis, S is the first moment of area above and about the centroidal axis, f_{ctm} is the concrete mean tensile strength, obtained according to EC2, and σ_{cp} is the concrete compressive stress at the centroidal axis due to prestress. The reduction factor, α_1, can be assumed as expressed in Eqn. 3.3, by assuming that the full development of the prestressing force is reached at 55 times the diameter of strands, according to a linear prestress distribution along strands. Furthermore, as evidenced by the performed campaign of refined monotonic non-linear solid finite element analyses, which highlighted that each considered specimen experienced the maximum shear stress overall the whole member for section at $0 < x/D < 0.5$, the considered critical section is fixed at one half of the slab depth. However, in this range ($0 < x/D < 0.5$), no significant difference was appreciated in terms of maximum shear stress experienced at different longitudinal distance from support. Additionally, it should be noticed that this reduction factor already assumes significantly low values, about 0.15-0.36, according to each hollow core slab depth; hence, assuming a further reduced critical section, would imply no evident variation in terms of predicted shear stress and, hence, shear strength capacity, due to the influence of the square root.

$$\alpha_1 = \frac{l_x}{l_{pt2}} = \frac{D}{2 \cdot 55\phi} \tag{3.3}$$

Particular care should be paid to the dimensionless local hollow core shape coefficient, C_{HCS}, defined according to Eqn. 3.4, to properly capture the influence of the different hollow core shapes, both circular and non-circular, on the shear strength capacity of the analysed hollow core floor slab units.

$$C_{HCS} = C_1\left(\frac{b_1}{r}\cdot C_2\frac{h_3}{r}\cdot C_3\frac{b_2}{b_1}\right) \qquad \text{where} \qquad \begin{cases} C_2\dfrac{h_3}{r}=1 & \text{if } \dfrac{h_3}{r}=0 \\ C_3\dfrac{b_2}{b_1}=1 & \text{if } \dfrac{b_2}{b_1}=0 \end{cases} \tag{3.4}$$

This local non-dimensional corrective factor, basically introduced according to the nominal hollow core shape parameters, describes the non-circularity level of each specimen and its local web width variation along the slab depth, based on dimensionless local coefficients. In fact, b_1/r can be defined as the ratio the horizontal distance between the webs and the void radius, while both h_3/r and b_2/b_1 represent the web width drop irregularity level, since h_3/r can be considered as a measure of the constant web width stretch extension along the depth and b_2/b_1 a direct dimensionless quantification of the abrupt and sharp web width drop, whereas an inclination of 45° is assumed. Additionally, three corrective safety factors, C_1=1.1, C_2 = 1 C_3 = 1.15, are introduced. It should be noticed that, if the considered specimen presents circular voids, b_1/r = 1 while h_3/r = 0, and, hence, it is set $C_2 \cdot h_3/r$ =1, in order not to cancel C_{HCS}. Similar consideration can be drawn if b_2 is null.
In Figure 3.2, the global, I and S, and local geometric parameters, b_w, b_1/r, h_3/r and b_2/b_1, adopted to define the proposed approach, are shown for each considered specimen class.
Therefore, to check and quantify the effectiveness of the proposed approach, varying depth and characteristics of voids, the shear strength capacity of the 49 specimens, tested at VTT, was predicted according to the proposed design method. The reliability of the alternative suggested expression, developed in compliance with local numerical evidences, deduced from the campaign of numerical finite element analyses, in terms of failure mechanism, crack pattern and shear stress distributions, is evaluated by comparing the predicted shear strength capacity with those experimentally observed [Pajari, 2005], and analytically predicted (EC2, Yang, ACI and CSA methods).

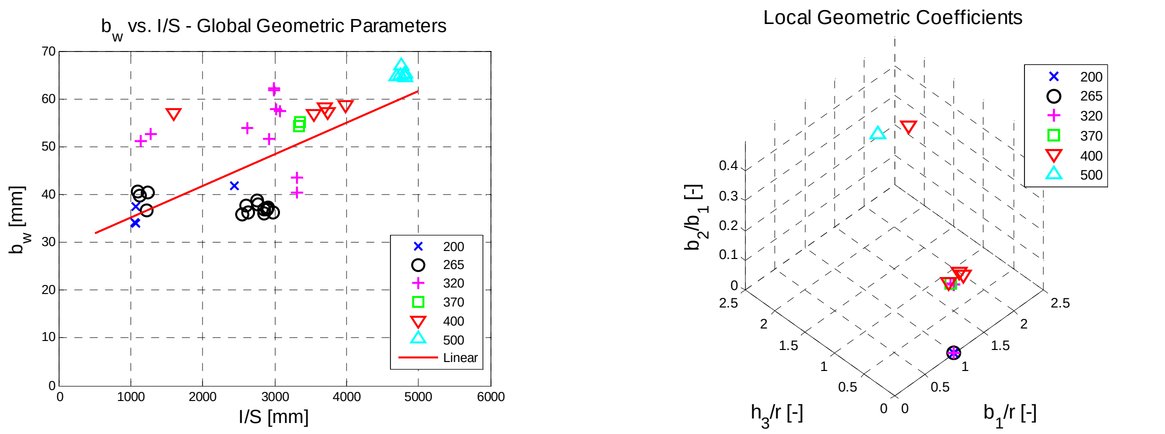

Figure 3.2 Specimens' global and local geometric parameters. b_w vs. I/S, b_2/b_1 vs. b_1/r and h_3/r, respectively

As highlighted in Figure 3.3, an improved agreement between experimental and analytical results, for each tested nominal depth, clearly emerges. Hence, this suggested method, based on the introduction of dimensionless corrective factors to suitably represent the local hollow core shape, which, according to the numerical analyses, controls the web-shear failure mechanism, seems to more properly capture experimental evidences, for hollow core units characterized by both circular and non-circular voids.

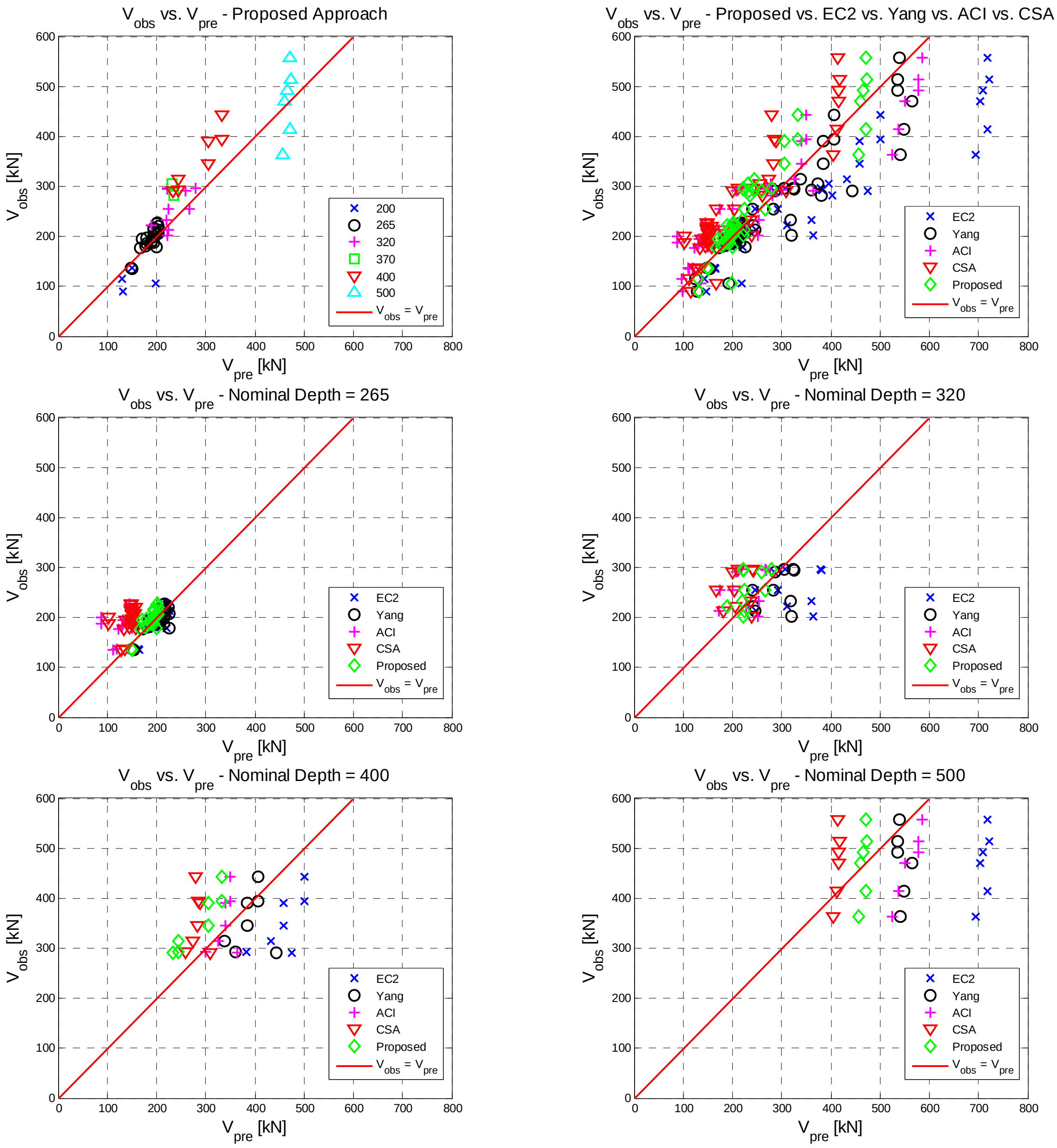

Figure 3.3 Proposed approach: experimentally observed, V_{obs}, vs. analytically predicted, V_{pre}, shear strength capacity, globally and separately compared with other analytical methods

The proposed approach still tends to provide unconservative predictions in case of 200 mm deep units, but it has to be highlighted that only four experimental tests are available. Conversely, the predicted shear strength capacity is more conservative than the EC2 approach, revealing a closer agreement with respect to Yang's design method. For what concerns CSA, safer, but still unconservative predictions are achieved, while, ACI provisions lead to a mean value approximately close to one, but with a standard deviation larger than 20%.

Since the experimental results of twenty tests on hollow core units characterized by a thickness of 265 mm are available, more reliable comparisons can be done in this case. The suggested alternative approach leads to slightly conservative predictions, characterized by an evidently increased accuracy level, if compared to the other investigated methods. In fact, the obtained mean value of the ratio between experimentally observed and predicted shear strength capacity is close to one, approximately 1.03, with a low standard deviation (7%). Conversely, both EC2 and Yang's methods tend to provide unsafe predictions, reaching values of 0.94 and 0.96, respectively, while both ACI and CSA prescriptions result in over-conservative evaluations, characterized by unacceptable inaccuracy levels (1.46 and 1.40, respectively) and inconsistent standard deviation (values higher than 20%).

The 320 mm thick hollow core slab units have been tested with both circular and non-circular voids, so the effects of different shapes can be studied. Effective predictions are achieved for both circular and non-circular hollow core slab units, if the suggested approach is adopted. In fact, mean values of the ratio between experimentally observed and predicted shear strength capacities close to one, in particular 1.04 for circular voids and 1.16 for non circular voids, are obtained with standard deviations of 9% and 18%. Consequently, if 320 mm deep specimens are globally considered, the alternative method leads to a mean ratio between observed and predicted shear strength capacity of about 1.10, with an acceptable standard deviation of 14%. The accuracy of the results is consistently increased if compared to each of the previously considered method. In fact, if circular hollow core specimens are considered, each adopted approach lead to trends in strong agreement with 265 mm deep units, again characterized by circular voids. Both EC2 and Yang methods provide slightly unconservative predictions with respect to the experimental results, reaching a mean ratio between observed and predicted shear strength capacity (0.95 and 0.96), while both ACI and CSA provisions result in evidently conservative and unacceptable predictions (1.35 and 1.37). On the contrary, considering non-circular voids specimens, both EC2 and Yang approaches leads to strongly unconservative estimations (0.69 and 0.82), while ACI provisions result in slightly unconservative predictions (0.98); only CSA method conduct to slightly safe analytically predicted shear strength capacities (1.07).
The effectiveness of the proposed method is more consistently validated in the case of 320 mm deep units with both circular and non-circular voids globally considered, since both EC2 and Yang provides a non conservative estimation of approximately 20%, while both ACI and CSA are more conservative than the suggested approach (5 and 10%, respectively), but with standard deviation higher than 20%.
For 370 mm deep non-circular voids hollow core slab units, the proposed alternative method provides slightly more conservative predictions in comparison with those obtained for 320 mm thick specimens, reaching ratios between experimentally observed and analytically predicted shear strength capacity ranging from 1.20 to 1.32; hence, slightly less accurate, anyway conservative results are achieved. However, more reliable considerations requires a larger experimental tests number and hence, it can be stated that only a tendency seems to be evident. If compared to the other investigated approaches, it should be noticed that both EC2 and Yang’s method provide evidently unsafe predictions, leading to an underestimation of the experimentally observed shear strength capacities of about 20%, while both ACI and CSA provisions allow for more accurate and slightly conservative predictions, evidencing a discrepancy between their prediction and the alternative approach of about 10%.
A satisfying fit with experimental results, characterized by a mean ratio of about 1.24, is achieved if the proposed approach is applied to 400 mm deep units. The comparisons between this method and the other approaches are similar to the results obtained in the previous cases. As before, EC2 provisions lead to a evidently non conservative prediction larger than 20%, while Yang’s method accuracy is consistently increased, anyway providing again unsafe predictions (0.91), with a standard deviation of 14%. Conversely, CSA leads to slightly more conservative predictions, in comparison with the alternative approach, anyway characterized by inconsistent standard deviation higher than 20%. Only ACI provides slightly conservative and more accurate results (1.05), if compared to the suggested method, anyway evidencing an increased standard deviation, of about 15%. From the comparison between the alternative method and ACI and CSA traditional approaches, it should be emphasized that ACI and CSA predictions ranges from 0.80 to 1.27 and from 0.94 to 1.59, respectively, while the proposed approach leads to results evidently closer to the theoretical model, from 1.13 to 1.33, for each specimen, providing a better fit with experimental results.
Safe predictions, evidently closer to the theoretical model, can be achieved if the alternative approach is applied to 500 mm deep non-circular voids hollow core slab units, characterized by a mean ratio between experimentally observed and analytically predicted shear strength capacity close to one and an acceptable standard deviation of 14%. Again, both EC2 and Yang methods provide tremendously unconservative results, evidencing a mismatch with the theoretical model larger than 30% and 15%, respectively. The adoption of these approaches leads to evidently unsafe predictions for each analysed specimen. Unlike before, either ACI provides unconservative predictions, of approximately 20% in terms of mean predicted shear strength capacity. Hence, only CSA prescriptions allow for safe predictions in terms of mean predicted shear strength capacity, anyway clearly more conservative, of approximately 13%, if compared to the suggested alternative method. Furthermore, increased standard deviation, larger than 15%, clearly emerges from CSA estimations. Finally, it should be noticed that a

satisfying, accurate, consistent and robust fit with experimentally predicted shear strength capacities is reached by adopting the proposed alternative approach.

Table 3.1 mean and standard deviation of the ratios between observed and predicted shear strength capacity, V_{obs}/V_{pre}, according to EC2, ACI, CSA provisions, Yang's method and proposed alternative approach

	Loss of prestress = 5%									
	EC2		**Yang**		**ACI**		**CSA**		**PROPOSED**	
Slab Type	Mean	St. dev	Mean	St. dev	Mean	St. dev	Mean	St. dev	Mean	St. dev
All	0.828	14.7%	0.905	12.2%	1.212	31.6%	1.248	24.6%	1.060	16.2%

If compared to other methods, the proposed alternative approach predictions are characterized by reduced or, at least, similar standard deviation, for each nominal depth considered. In fact, both ACI and CSA provisions, usually tend to provide predictions characterized by higher standard deviations, larger than 20%, in comparison with EC2 and Yang's approach. This trend is particularly evident for reduced depth hollow core units with circular voids. Therefore, a better fit with experimental data, almost similar and uniform for each considered nominal depth, unlike the EC2, Yang, ACI and CSA, which achieve varying levels of accuracy, according to different nominal depths and hollow core shapes, with circular and non-circular voids. Finally, it should be evidenced that the simple alternative approach seems to provide an accurate, slightly conservative and consistent agreement with experimentally observed shear strength capacities for each type of considered depth, cross-sectional geometric features, hollow core shape and configuration, circular and non-circular, regularity of web width variation along slab depth, steel strands arrangement and loading configuration. In fact, according to the obtained mean values, close to one, and standard deviations, of about 15%, a reliable match between analytical predictions and experimental evidences emerges, while the other methods seem to be characterized by unconservative mismatch (EC2 and Yang) or over-conservative and scattered predictions (ACI and CSA), evidencing particularly critical scenario, if adopted out of their implicit field of applicability.

4 CONCLUSIONS

The performed campaign of non-linear solid finite element analyses evidenced the dependency of the experienced brittle web-shear failure mechanism with respect to hollow core shape and relative web width variation along slab depth. The proposed analytical approach, based on maximum principal tensile stress criterion failure, Mohr's circle theory and isotropic concrete behaviour, combined with the introduction of dimensionless corrective local geometric coefficients, able to capture the effect of the hollow core shape, particularly in terms of web width variation along depth, leads to an accurate, slightly conservative and consistent agreement with experimentally observed shear strength capacities.

REFERENCES

ACI Committee (2005). Building Code Requirements for Structural Concrete (ACI 318-05) and Commentary (ACI 318R- 05), *American Concrete Institute*, Farmington Hills, MI.
Bentz, E.C., Vecchio, F.J. and Collins, M.P. (2006). Simplified Modified Compression Field Theory for Calculating Shear Strength of Reinforced Concrete Elements. *ACI Structural Journal* **103:S65**, 614-624.
Canadian Standards Association (2001). CSA Standard A23.3-04, Design of Concrete Structures.
Commission for the European Communities, Eurocode 2 [2005]: Design of Concrete Structures – Part 1: General Rules and Rules for Buildings, EN 1992-1-1.
Hawkins, N.M. and Ghosh, S.K. (2006). Shear Strength of Hollow Core Slabs. *PCI Journal* **51:1**,110-114.
Pajari, M. (2005). Resistance of Prestressed Hollow Core Slabs Against Web Shear Failure. Research Notes 1292, VTT Building and Transport.
Yang, L. (1994). Design of Prestressed Hollow Core Slabs with Reference to Web Shear Failure. *Journal of Structural Engineering ASCE* **120:9**, 2675-2696.